



City Research Online

City, University of London Institutional Repository

Citation: Giaralis, A. & Spanos, P. D. (2010). Effective linear damping and stiffness coefficients of nonlinear systems for design spectrum based analysis. *Soil Dynamics and Earthquake Engineering*, 30(9), pp. 798-810. doi: 10.1016/j.soildyn.2010.01.012

This is the unspecified version of the paper.

This version of the publication may differ from the final published version.

Permanent repository link: <http://openaccess.city.ac.uk/920/>

Link to published version: <http://dx.doi.org/10.1016/j.soildyn.2010.01.012>

Copyright and reuse: City Research Online aims to make research outputs of City, University of London available to a wider audience. Copyright and Moral Rights remain with the author(s) and/or copyright holders. URLs from City Research Online may be freely distributed and linked to.

City Research Online:

<http://openaccess.city.ac.uk/>

publications@city.ac.uk

EFFECTIVE LINEAR DAMPING AND STIFFNESS COEFFICIENTS OF NONLINEAR SYSTEMS FOR DESIGN SPECTRUM BASED ANALYSIS

Agathoklis Giaralis¹ and Pol D. Spanos^{2*}

¹School of Engineering and Mathematical Sciences, City University London, Northampton Square, EC1V 0HB, London, UK. E-mail: agathoklis@city.ac.uk

²L. B. Ryon Chair in Engineering, Rice University, MS 321, P.O. Box 1892, Houston, TX 77251, USA. E-mail: spanos@rice.edu

ABSTRACT

A stochastic approach for obtaining reliable estimates of the peak response of nonlinear systems to excitations specified via a design seismic spectrum is proposed. This is achieved in an efficient manner without resorting to numerical integration of the governing nonlinear equations of motion. First, a numerical scheme is utilized to derive a power spectrum which is compatible in a stochastic sense with a given design spectrum. This power spectrum is then treated as the excitation spectrum to determine effective damping and stiffness coefficients corresponding to an equivalent linear system (ELS) via a statistical linearization scheme. Further, the obtained coefficients are used in conjunction with the (linear) design spectrum to estimate the peak response of the original nonlinear systems. The cases of systems with piecewise linear stiffness nonlinearity, along with bilinear hysteretic systems are considered. The seismic severity is specified by the elastic design spectrum prescribed by the European aseismic code provisions (EC8). Monte Carlo simulations

pertaining to an ensemble of non-stationary EC8 design spectrum compatible accelerograms are conducted to confirm that the average peak response of the nonlinear systems compare reasonably well with that of the ELS, within the known level of accuracy furnished by the statistical linearization method. In this manner, the proposed approach yields ELS which can replace the original nonlinear systems in carrying out computationally efficient analyses in the initial stages of the aseismic design of structures under severe seismic excitations specified in terms of a design spectrum.

Keywords: Statistical linearization, design spectrum, inelastic spectrum, bilinear hysteretic, equivalent linear system, power spectrum

1. INTRODUCTION

Contemporary code provisions favor response spectrum-based analyses for the aseismic design of structures. For this purpose, they prescribe elastic response (design) spectra to define the input seismic severity in terms of the peak response of linear single-degree-of-freedom (SDOF) oscillators characterized by their natural period T and ratio of critical damping ζ (e.g. [1]). Nevertheless, regulatory agencies allow for ordinary structures to exhibit inelastic/hysteretic behavior (i.e. to suffer some structural damage), towards achieving cost-effective, functional, and aesthetically acceptable designs. In a performance-based design context, the extent of the allowable damage depends on the severity of the seismic event considered relative to the one defined by the elastic design spectrum (e.g. [2]). This is accomplished, within the

common force-based aseismic design procedure, by considering reduced input seismic forces compared to those prescribed by the elastic design spectrum by a factor R (strength reduction factor), with the stipulation that appropriate detailing is ensured during construction so that the structure complies with certain “performance criteria”. Inherent to the latter consideration is the concept of ductility demand μ which is equal to the ratio of the maximum lateral deformation attained by a yielding structure over a “nominal” yielding deformation. Thus, linear response spectrum-based analysis can still be applied for the aseismic design of ordinary constructed facilities by incorporating a spectrum of reduced ordinates (inelastic design spectrum) to allow for inelastic structural behavior expressed in terms of a specified level of ductility demand.

Initiated by the work of Veletsos and Newmark [3], significant research effort has been devoted over the past five decades to calculating the peak response of SDOF oscillators of T natural period for small oscillations (i.e. when no yielding occurs) tracing various nonlinear force-deformation laws for a large number of recorded ground motions pertaining to various seismic events. This is done by numerical integration of the governing nonlinear equations of motion. Based on such extensive numerical studies, several semi-empirical R - μ - T relations have been proposed for obtaining inelastic response spectra from the elastic ones (see e.g. References [4-7]). In fact, all contemporary code provisions rely on simplified versions of such relations to define inelastic response spectra to be used for the design of structures.

Alternatively, computationally demanding inelastic time-history analyses can be incorporated to obtain the inelastic response time-histories of nonlinear structures using numerical integration techniques. In the aseismic design framework dictated by a specific code, these kinds of analyses require the consideration of field recorded or artificially generated

seismic accelerograms conforming with certain compatibility criteria with the prescribed elastic design spectrum (see e.g. [8]).

A considerably different approach in dealing with nonlinear systems response determination is to employ a linearization technique. That is, to approximate the *a priori* unknown response of the nonlinear systems by considering the response of an appropriately defined “equivalent” linear system (ELS). In general, the dynamical properties of the ELS (effective/equivalent stiffness and damping) depend on the force-deformation law of the nonlinear system (e.g. elastic, inelastic/ hysteretic), on the input excitation (e.g. harmonic, earthquake, stochastic etc.), and on the various assumptions made by the particular linearization scheme. Representing a non-linear oscillator by a linear effective natural period T_{eq} and a ratio of critical damping ζ_{eq} facilitates the study of the underlying non-linear behavior significantly since these effective linear properties are amenable to a clear physical interpretation. More importantly, in obtaining the response of the nonlinear system the numerical integration of the nonlinear equations of motion is circumvented by such a representation. This of course is achieved at the cost of accepting certain errors due to the simplifying approximating assumptions inherent to all linearization techniques. For instance, in the cases where the response of nonlinear SDOF and multi-DOF systems to a stochastic excitation is of interest, the method of statistical (or stochastic) linearization is considered the most versatile alternative to the computationally demanding Monte Carlo analyses (see e.g. [9] and references therein). The latter analyses involve the integration of the nonlinear equations deterministically for an appropriately derived ensemble of time-histories statistically consistent with the considered stochastic input process.

Focusing on earthquake engineering applications, consideration of equivalent linear oscillators derived from non-linear oscillators allows for interpreting the inelastic response

spectra as elastic response spectra corresponding to the effective stiffness and damping properties of the ELS (e.g. [10]). In fact, this interpretation renders possible the development of inelastic spectra from (T_{eq}, ζ_{eq}) - μ - T relations as opposed to the previously discussed R- μ - T relations. For example, Iwan and Gates [11] and Kwan and Billington [12] derived (T_{eq}, ζ_{eq}) - μ - T relations via numerical integration of various non-linear oscillators exposed to certain field recorded strong ground motions. Furthermore, Gulkan and Sozen [13] and Shibata and Sozen [14] suggested the use of ELS, derived from pertinent experimental results on single and multi storey R/C frames, as a tool for aseismic design of R/C structures. Based on the above concepts, the tool of an equivalent linear SDOF “substitute” structure is incorporated to account for the inelastic behavior of SDOF and MDOF structures in various contemporary methodologies for the aseismic design and the assessment of the seismic vulnerability of structures (see e.g. [15-18]). Clearly, the development of efficient linearization schemes accounting for the input seismic action in terms of a given design spectrum is critical and timely.

Jennings [19] considered and compared six early deterministic linearization methods, assuming harmonic excitation and steady-state response conditions. Further, Iwan and Gates [20] assessed the potential of various linearization techniques to estimate the peak response of certain SDOF hysteretic oscillators exposed to strong ground motion. This was done vis-à-vis numerical results obtained by integrating the nonlinear equations of motion for an ensemble of 12 recorded accelerograms. Similarly, Hadjian [21] compared the formulae for defining equivalent linear properties resulting from several linearization techniques for elasto-plastic SDOF hysteretic systems. All the linearization techniques considered in these early studies define deterministically the ELSs without considering the statistical attributes of the seismic hazard explicitly.

More recently, Koliopoulos et al. [22] pursued a comparative assessment of the applicability of certain linearization schemes for the case of bilinear hysteretic SDOF systems. In this case a small ensemble (9) of artificial accelerograms whose average response spectra was relatively close to a specific design spectrum prescribed by the European aseismic code provisions (EC8) was used for the numerical validation of the techniques considered. One of these schemes involved random vibration-based linearization relying on the solution of an underlying Fokker-Planck equation, necessitating the assumption of white noise input: a limiting one for representing strong ground motion excitations.

Furthermore, Basu and Gupta [23] derived inelastic spectra pertaining to certain recorded seismic accelerograms also based on a statistical linearization formulation. This formulation required the minimization of the expected value of the square difference (error) between the considered nonlinear equation of motion and the corresponding (target) equivalent linear with respect to the dynamical properties of the ELS. The associated expected values were computed based on the distribution of the peak response of the ELS excited by a Gaussian stationary process. A piecewise linear non-hysteretic type of nonlinearity was considered with a fixed value for the yielding displacement selected so that the system experiences mild nonlinear behavior. An attempt to predict the lower order displacement peaks and to develop constant cumulative damage spectra was also made assuming a Kanai-Tajimi filtered white noise excitation. Later, the formulation was applied for the case of bilinear hysteretic oscillators [24]. However, the scope of both of the aforementioned studies was to estimate the damage accumulation of the underlying nonlinear systems. Thus not special attention was given to the equivalent linear parameters which were treated as by-products of the statistical linearization formulation followed.

Moreover, in Miranda and Ruiz-García [25] the performance of four deterministic linearization schemes, along with two popular $R-\mu-T$ relations, were evaluated to obtain peak deformations of certain hysteretic SDOF systems. Special attention was given to quantifying the error of the estimated maximum responses versus results from a comprehensive Monte Carlo analysis involving the numerical integration of the nonlinear systems for a bank of 264 recorded accelerograms.

In a study concerning the response of secondary systems founded on SDOF nonlinear systems, Politopoulos and Feau [26] proposed two different schemes to derive equivalent linear parameters. The first, concerns hysteretic perfectly elasto-plastic SDOF systems and involves a least square fit of linear transfer functions to power spectra estimated from response data of nonlinear systems obtained from Monte Carlo analyses. Clearly, this procedure does not circumvent the numerical integration of the nonlinear equations of motion while it involves certain approximations associated with spectral estimation and curve fitting considerations. The second, pertains to a class of nonlinear elastic systems subject to white noise excitation and utilizes a special statistical linearization procedure treating the equivalent linear stiffness parameter as a random variable. From a practical viewpoint, both the white noise excitation assumption and the probabilistic nature of the equivalent linear stiffness parameter considered limit, rather significantly, the merit of these proposed linearization methods.

Notably, the potential advantages of focusing on the ELS derived from the method of statistical linearization considering input processes consistent with elastic design spectra seems to have been overlooked in the published literature. In this paper, a design spectrum compatible power spectrum is considered in conjunction with appropriate statistical linearization schemes as a surrogate for determining the peak seismic response of nonlinear systems. It is emphasized that

the purpose of the present work is not to assess the accuracy of the statistical linearization technique, a well-studied theme in the literature (see e.g [9] and references therein). Instead, it proposes a novel approach to estimate inelastic response spectral ordinates from a given family of elastic spectra for various damping ratios without resorting to numerical integration of the underlying nonlinear equations of motion. In this manner, the need to consider field recorded accelerograms of similar characteristics to the ones that have been used in the definition of the considered design spectrum is circumvented. Furthermore, the inherent probabilistic nature of the excitation is explicitly accounted for. Note that the stationarity assumption in the surrogate model of the strong ground motion input renders the statistical linearization step quite efficient, while it is not particularly restrictive in accounting for the physical aspects of strong ground motions. In fact, it has been argued that stationary power spectra consistent with a given response/design spectrum accounts implicitly for the transient attributes of the response of seismically excited structures as these reflect on the response/design spectrum [27].

Figure 1.

For clarity, the proposed approach is qualitatively presented in the flowchart of Figure 1. Clearly, the main steps of the approach encompass the derivation of a design spectrum compatible power spectrum, an issue that has been extensively studied in the open literature (e.g. [28-31]), and the application of the statistical linearization method (see e.g. [9, 32-33]). To this end, in section 2 an efficient method for deriving design spectrum compatible power spectrum is considered. Further, section 3 reviews the pertinent mathematical formulae for deriving ELS via the statistical linearization method for viscously damped SDOF oscillators characterized by hardening piecewise linear elastic, and bilinear hysteretic restoring force-deformation laws. Section 4 provides numerical results supporting the effectiveness and the practical usefulness of

the proposed approach in conjunction with the design spectrum prescribed by EC8 [2]. Finally, section 5 includes pertinent concluding remarks.

2. DERIVATION OF RESPONSE SPECTRUM COMPATIBLE POWER SPECTRA

The core equation for relating a design/response pseudo-acceleration seismic spectrum S_a to a one-sided power spectrum $G(\omega)$ representing a Gaussian stationary process $g(t)$ in the frequency domain reads (e.g. [34])

$$S_a(\omega_j, \zeta_n) = \eta_{j,G} \omega_j^2 \sqrt{\lambda_{j,0,G}}. \quad (1)$$

In the above equation $\lambda_{j,m,G}$ denotes the spectral moment of order m of the stationary response of a linear single-degree-of-freedom (SDOF) mass-spring-damper system of natural frequency ω_j and damping ratio ζ_n base-excited by the process $g(t)$. Namely,

$$\lambda_{j,m,G} = \int_0^{\infty} \frac{\omega^m G(\omega)}{(\omega^2 - \omega_j^2)^2 + (2\zeta_n \omega \omega_j)^2} d\omega. \quad (2)$$

Furthermore, the “peak factor” $\eta_{j,G}$ appearing in Equation (1) is the critical parameter establishing the equivalence, with probability of exceedance p , between the S_a and $G(\omega)$ [34]. Specifically, it represents the factor by which the standard deviation of the response of the considered SDOF oscillator must be multiplied to predict the level S_a below which the peak response of the oscillator will remain, with probability p , throughout the duration of the input process T_s . The exact determination of $\eta_{j,G}$ is associated with the first passage problem which involves the evaluation of the probability that the response of a linear SDOF oscillator does not cross a certain amplitude level (barrier) within the duration T_s (see e.g. [35]). A closed form solution for this problem is not available. Herein, the following semi-empirical formula for the

calculation of the peak factor is adopted which is known to be reasonably reliable for earthquake engineering applications ([34, 36])

$$\eta_{j,G} = \sqrt{2 \ln \left\{ 2v_{j,G} \left[1 - \exp \left(-q_{j,G}^{1.2} \sqrt{\pi \ln(2v_{j,G})} \right) \right] \right\}}, \quad (3)$$

where

$$v_{j,G} = \frac{T_s}{2\pi} \sqrt{\frac{\lambda_{j,2,G}}{\lambda_{j,0,G}}} (-\ln p)^{-1}, \quad (4)$$

and

$$q_{j,G} = \sqrt{1 - \frac{\lambda_{j,1,G}^2}{\lambda_{j,0,G} \lambda_{j,2,G}}}. \quad (5)$$

For the purposes of this study, it is appropriate to set the probability p equal to 0.5 in Equation (4). Under this assumption, Equation (1) prescribes the following compatibility criterion: considering an ensemble of stationary samples of the process $g(t)$ half of the population of their response spectra will lie below S_a (i.e. S_a is the median response spectrum). A computationally efficient numerical scheme is used to derive a non-parametric power spectrum $G(\omega)$ satisfying the aforementioned criterion for a given pseudo-acceleration design spectrum by solving the “inverse” stochastic dynamics problem governed by Equations (1) to (5). Compared to other methods utilized in the literature in a similar context, this scheme does not require iterations to be performed as in [28-29], and does not involve the solution of an optimization problem as in [29-30].

In particular, the adopted scheme relies on the following approximate formula to obtain a reliable estimate for the response variance of a lightly damped SDOF system subject to a relatively broadband excitation [34]

$$\lambda_{j,0,G} = \frac{G(\omega_j)}{\omega_j^3} \left(\frac{\pi}{4\zeta_n} - 1 \right) + \frac{1}{\omega_j^4} \int_0^{\omega_j} G(\omega) d\omega. \quad (6)$$

Approximating the integral in Equation (6) by a discrete summation, substituting Equation (6) in Equation (1), and appropriately rearranging the resulting terms yields [31, 34]

$$G[\omega_j] = \begin{cases} \frac{4\zeta}{\omega_j \pi - 4\zeta_n \omega_{j-1}} \left(\frac{S_\alpha^2(\omega_j, \zeta_n)}{\eta_{j,N}^2} - \Delta\omega \sum_{k=1}^{j-1} G[\omega_k] \right), & \omega_j > \omega_0 \\ 0, & 0 \leq \omega_j \leq \omega_0 \end{cases}. \quad (7)$$

The latter equation establish an approximate numerical scheme to recursively evaluate $G(\omega)$ at a specific set of equally spaced by $\Delta\omega$ (in rad/sec) natural frequencies $\omega_j = \omega_0 + (j-0.5)\Delta\omega$; $j=1, 2, \dots, M$ where ω_0 denotes the lowest bound of the existence domain of Equation (3) [31]. Specifically, ω_0 should be set equal to the lowest value of the natural frequency ω_n which simultaneously satisfies the conditions

$$\ln(2v_{j,N}) \geq 0, \quad (8)$$

and

$$\ln \left\{ 2v_{j,N} \left[1 - \exp \left(-q_{j,N}^{1.2} \sqrt{\pi \ln(2v_{j,N})} \right) \right] \right\} \geq 0. \quad (9)$$

Obviously, in implementing the above scheme the peak factors $\eta_{j,N}$ need to be calculated for an input power spectrum $N(\omega)$ which has to be *a priori* assumed without knowledge of $G(\omega)$. The duration of the underlying stationary process characterized by $N(\omega)$ is assumed equal to the duration T_s of $g(t)$. Conveniently, the value of $\eta_{j,N}$ is not very sensitive to the shape of the spectrum $N(\omega)$ (see e.g. [36]). This observation is justified by the fact that the evaluation of the peak factor (Equations (2) to (5)), involves ratios of integrals of the product of the input power spectrum with the squared modulus of the frequency response function of the various SDOF systems considered over the whole range of frequencies. The validity of this assertion is verified

in a following section using numerical results pertaining to three different shapes of $N(\omega)$. These are the unit amplitude white noise (WN) spectrum

$$N(\omega) = 1 \quad ; \quad 0 \leq \omega \leq \omega_b, \quad (10)$$

the Kanai-Tajimi (KT) spectrum [37]

$$N(\omega) = \frac{1 + 4\zeta_g^2 \left(\frac{\omega}{\omega_g}\right)^2}{\left(1 - \left(\frac{\omega}{\omega_g}\right)^2\right)^2 + 4\zeta_g^2 \left(\frac{\omega}{\omega_g}\right)^2} \quad ; \quad 0 \leq \omega \leq \omega_b, \quad (11)$$

and the Clough-Penzien (CP) spectrum [38]

$$N(\omega) = \frac{\left(\frac{\omega}{\omega_f}\right)^4}{\left(1 - \left(\frac{\omega}{\omega_f}\right)^2\right)^2 + 4\zeta_f^2 \left(\frac{\omega}{\omega_f}\right)^2} \frac{1 + 4\zeta_g^2 \left(\frac{\omega}{\omega_g}\right)^2}{\left(1 - \left(\frac{\omega}{\omega_g}\right)^2\right)^2 + 4\zeta_g^2 \left(\frac{\omega}{\omega_g}\right)^2} \quad ; \quad 0 \leq \omega \leq \omega_b, \quad (12)$$

where ω_g , ζ_g , ω_f , and ζ_f are predefined constant parameters, and ω_b is the largest frequency of interest. The values of the parameters ω_g , ζ_g reflect the filtering effects of the surface soil deposits on the propagating seismic waves during an earthquake event. Thus, they should be judiciously chosen based on the soil conditions associated with the given (target) design spectrum. The parameters ω_f , ζ_f control the shape of the high-pass filter incorporated in the CP spectrum to suppress the low frequencies allowed by the KT spectrum and their values should be selected accordingly. More detailed discussions on the spectral forms of Equations (11) and (12) can be found in [8] and the references therein.

To this end, it is noted that the evaluation of the spectral moment integrals defined by Equation (2) for the input spectra given by the Equations (10) to (12) can be performed either numerically using appropriate quadrature rules or analytically. In the latter case, the residue

theorem for complex integration can be employed [36]. Alternatively, these response spectral moments can be obtained by solving linear systems of equations derived from application of the Hilbert transform on the governing differential equations of motion as it has been shown by Spanos and Miller [39]. For the simplest case of $N(\omega)$ being unit strength white noise (WN) the following closed form expressions for the quantities in Equations (4) and (5) hold

$$v_{j,N=1} = \frac{T_s}{2\pi} \omega_{n(j)} (-\ln p)^{-1}, \quad (13)$$

$$q_{j,N=1} = \sqrt{1 - \frac{1}{1-\zeta^2} \left(1 - \frac{2}{\pi} \tan^{-1} \frac{\zeta}{\sqrt{1-\zeta^2}} \right)^2}. \quad (14)$$

Regarding the conditions of Equations (8) and (9), pertinent plots shown in Figure 2(a) reveal that Equation (9) defines a more stringent criterion which is satisfied for relatively small values of ω_0 for the cases that $N(\omega)$ assumes a WN and a KT spectral form (Figure 2(b)). Results from extensive numerical experimentation, similar to those presented in Figure 1 indicate that for the range of values of the KT parameters, ω_g and ζ_g , of practical interest, the admissible values for ω_0 coincide with those for the WN input spectrum. Interestingly, for the CP spectrum ω_0 is always zero since the left hand side of Equations (8) and (9) are positive everywhere (see also Figure 2(a)). This result is associated with the fact that the CP spectrum vanishes as $\omega \rightarrow 0$.

Figure 2.

Note that upon determining the discrete power spectrum $G[\omega_j]$ by Equation (7) the associated pseudo-acceleration response spectrum $D[\omega_j, \zeta]$ can be computed in a straightforward manner using Equations (1) to (5). For this purpose, the first three spectral moments of the

response of a SDOF system excited by a process characterized by a power spectrum known at equally spaced frequencies can be evaluated by the formulas reported in [29, 40], which are included in the Appendix for completeness.

Incidentally, if so desired, the initially obtained discrete power spectrum $G[\omega_j]$ can be further modified iteratively to improve the matching of the associated response spectrum $D[\omega_j, \zeta]$ with the target design spectrum S_α according to the equation written at the ν -th iteration (e.g. [27])

$$G^{(\nu+1)}[\omega_j] = G^{(\nu)}[\omega_j] \left(\frac{S_\alpha[\omega_j, \zeta]}{D^{(\nu)}[\omega_j, \zeta]} \right)^2. \quad (15)$$

3. BACKGROUND ON THE STATISTICAL LINEARIZATION METHOD

Consider a unit-mass viscously-damped quiescent SDOF system with a non-linear restoring force component base-excited by the stationary zero-mean acceleration process $g(t)$ characterized in the frequency domain by the power spectrum $G(\omega)$. The equation of motion of this system reads

$$\ddot{x}(t) + 2\zeta_n \omega_n \dot{x}(t) + \omega_n^2 \varphi(x, \dot{x}) = -g(t) \quad ; \quad x(0) = \dot{x}(0) = 0, \quad (16)$$

in which $x(t)$ is the system deformation (displacement trace of the system relative to the motion of the ground), ω_n is the system natural frequency for small deformations, ζ_n is the ratio of critical viscous damping, and $\varphi(x, \dot{x})$ is a nonlinear function governing the restoring force-deformation law; the dot over a symbol signifies differentiation with respect to time t .

The statistical linearization method utilizes the response process y of an equivalent linear system (ELS) of natural frequency ω_{eq} and damping ratio ζ_{eq} given by the equation

$$\ddot{y}(t) + 2\zeta_{eq}\omega_{eq}\dot{y}(t) + \omega_{eq}^2 y(t) = -g(t) \quad ; \quad y(0) = \dot{y}(0) = 0, \quad (17)$$

to approximate the process x , that is, the response of the non-linear oscillator of Equation (16) [9]. According to the original and most widely-used form of statistical linearization the above linear system is defined by minimizing the expected value of the difference (error) between Equations (16) and (17) in a least square sense with respect to the quantities ω_{eq} and ζ_{eq} (i.e. the effective dynamical properties of the ELS), (see e.g. [9, 32-33]). This criterion yields the following expressions for the effective linear properties [9]

$$\omega_{eq}^2 = \frac{E\{x\varphi(x, \dot{x})\}}{E\{x^2\}}, \quad (18)$$

and

$$\zeta_{eq} = \zeta_n \frac{\omega_n}{\omega_{eq}} + \frac{E\{\dot{x}\varphi(x, \dot{x})\}}{E\{\dot{x}^2\}}, \quad (19)$$

where $E\{\cdot\}$ denotes the mathematical expectation operator. In this junction, it is commonly assumed that the unknown distribution of the response process x of the non-linear oscillator can be approximated, for the purpose of evaluating the expected values, by a zero-mean Gaussian process. Furthermore, it is also assumed that the variances of the processes x and y are equal ([9, 33]). The latter suggests that

$$E\{x^2\} = \lambda_{eq,0,G} = \int_0^{\infty} \frac{G(\omega)}{(\omega^2 - \omega_{eq}^2)^2 + (2\zeta_{eq}\omega\omega_{eq})^2} d\omega, \quad (20)$$

and

$$E\{\dot{x}^2\} = \lambda_{eq,2,G} = \int_0^{\infty} \frac{\omega^2 G(\omega)}{(\omega^2 - \omega_{eq}^2)^2 + (2\zeta_{eq}\omega\omega_{eq})^2} d\omega \quad (21)$$

in Equations (18) and (19). Under the aforementioned assumptions, Equations (18) and (19) can be simplified as [9]

$$\omega_{eq}^2 = E \left\{ \frac{\partial \varphi(x, \dot{x})}{\partial x} \right\}, \quad (22)$$

and

$$\zeta_{eq} = \zeta_n \frac{\omega_n}{\omega_{eq}} + E \left\{ \frac{\partial \varphi(x, \dot{x})}{\partial \dot{x}} \right\}. \quad (23)$$

For many nonlinear force-deformation laws of practical interest the above formulae assumption leads to closed-form expressions which facilitate significantly the application of the statistical linearization method [9]. In any case, Equations (20) to (23) establish a system of nonlinear equations that needs to be simultaneously satisfied. Typically, this is achieved via a numerical iterative scheme [9]. Conveniently for the purposes of the proposed approach, $G(\omega)$ is a non-parametric power spectrum known at a specific set of equally-spaced frequencies and thus the integrals in Equations (22) and (23) can be evaluated at each iteration using the closed-form formulas included in the Appendix.

It is noted that statistical linearization formulations using alternative criteria to minimize the error between Equations (16) and (17) have been proposed in the literature (e.g. [23, 33, 41-43]), while significant research effort has been also devoted in relaxing the aforementioned Gaussian distribution assumption (e.g. [44, 45]). However, such considerations involve computationally intensive iterative numerical schemes requiring the calculation of integrals which are not amenable to analytical treatment, without necessarily yielding results of substantially increased accuracy (see e.g. [23, 33, 43]). Since simplicity and computational efficiency are primary objectives in the herein proposed approach, the classical statistical linearization method is adopted in all of the ensuing analytical and numerical results to obtain

equivalent linear properties by minimizing the squared difference between the nonlinear and the equivalent linear system. Further, the assumption that the distribution of the nonlinear response can be approximated by a Gaussian one is adopted to compute the mathematical expectations in Equations (22) and (23). It should be clear from the preceding comments that the effective linear properties ω_{eq} and ζ_{eq} obtained through iterative solution of Equations (20) to (23) depend explicitly on the input power spectrum $G(\omega)$. In the framework of the proposed approach $G(\omega)$ is compatible with a given design spectrum and thus these ω_{eq} and ζ_{eq} are related in a statistical sense with the latter spectrum in a straightforward manner. This constitutes the main advantage of the herein developed approach over the common equivalent linearization techniques used in various aseismic design procedures which define ELSs without accounting for the input seismic action as defined by regulatory agencies by means of design spectra (see e.g. [18, 46-48]). In the remainder of this section certain nonlinear restoring force-deformation laws of practical interest are discussed, and the pertinent formulas to obtain the related ω_{eq} and ζ_{eq} are reported.

3.1. Piecewise linear restoring force

Consider a hardening non-linear elastic oscillator characterized by a piecewise linear restoring force consisted of two branches. Let $\alpha > 1$ be the stiffness (rigidity) ratio between the branches and x_y be the critical deformation for which a change of stiffness occurs as shown in Figure 3(a). The equation of motion for such a system is obtained by substituting in Equation (16):

$$\varphi(x) = \begin{cases} x & ; |x| \leq x_y \\ ax + \text{sgn}(x)x_y(1-\alpha) & ; \text{sgn}(x)x > x_y \end{cases}, \quad (24)$$

where $\text{sgn}(\bullet)$ symbolizes the signum function, namely, $\text{sgn}(x)= 1$ for $x>0$ and $\text{sgn}(x)= -1$ for $x<0$.

Figure 3.

In practical terms, the restoring force of Equation (24) can be considered in the context of preliminary aseismic design procedures in several cases. These include accounting for the pounding/impact effect in structural members such as between deck elements at expansion joints along the longitudinal direction of bridges (e.g. [49]), and between adjacent buildings (e.g. [50-51]). They also include cases of structures whose lateral movement is restricted via “stop-supports” and restrainers such as in above-ground pipelines along their transversal direction (e.g. [52]), and in seismically isolated structures (e.g. [53]). In this respect, the deformation x_y is construed as the clearance/distance between structural members or between structures and their surroundings, while the ratio α reflects the increase in the overall structural stiffness after impact.

Substitution of Equation (24) in Equations (22) and (23) yield the following expressions for the parameters of the ELS associated with a nonlinear oscillator with piecewise linear restoring force

$$\omega_{eq}^2 = \omega_n^2 \left(a + (1-a) \text{erf} \left(\frac{x_y}{\sqrt{2\lambda_{eq,0,G}}} \right) \right), \quad (25)$$

and

$$\zeta_{eq} = \zeta \frac{\omega_n}{\omega_{eq}}, \quad (26)$$

in which $\text{erf}(\bullet)$ denotes the error function defined as

$$\operatorname{erf}(u) = \frac{2}{\sqrt{\pi}} \int_0^u \exp(-v^2) dv. \quad (27)$$

Clearly, given a certain nonlinear oscillator with piecewise linear restoring force defined by a set of values for ω_n , ζ_n , a , and x_y or equivalently R (see Figure 3(a)), excited by a specific design spectrum compatible $G(\omega)$, a set of linear parameters ω_{eq} and ζ_{eq} can be computed by iteratively solving Equations (20), (25), and (26) [9].

3.2. Bilinear hysteretic restoring force

Of particular interest in the aseismic design of structures is the bilinear hysteretic force-deformation law show in Figure 3(b) which is the simplest model to capture the hysteretic behavior of structural members and structures under seismic excitation (see e.g. [7, 11, 14, 51, 54]). For instance, it is a common practice to model the inelastic behavior of structures, including multi-storey buildings and bridges, exposed to strong ground motion by viscously damped bilinear hysteretic SDOF oscillators in the context of non-linear static analyses (see e.g. [18, 47]) and of performance/displacement-based design procedures (e.g. [15-17]). The governing equation of motion of such an oscillator can be mathematically expressed with the aid of an auxiliary state z by substituting in Equation (16) [55]

$$\varphi(x, \dot{x}) = ax + (1-a)z, \quad (28)$$

where

$$\dot{z}(x, \dot{x}) = \dot{x} \left[1 - U(\dot{x})U(z - x_y) - U(-\dot{x})U(-z - x_y) \right], \quad (29)$$

in which x_y is the yielding deformation and $\alpha < 1$ is the post-yield to pre-yield (rigidity) ratio, and $U(\bullet)$ denotes the Heaviside step function, namely, $U(v) = 1$ for $v \geq 0$, and $U(v) = 0$ for $v < 0$.

Adopting the assumptions of the classical statistical linearization method and assuming that the response of the nonlinear system is narrowband (i.e. is dominated by a slowly varying in time apparent frequency) effective parameters of an ELS corresponding to a given viscously damped bilinear hysteretic SDOF system, are obtained via the formulae (e.g. [9, 32])

$$\omega_{eq}^2 = \omega_n^2 \left\{ 1 - \frac{8(1-a)}{\pi} \int_1^{\infty} \left(\frac{1}{v^3} + \frac{1}{\theta v} \right) \sqrt{v-1} \exp\left(\frac{-v^2}{\theta}\right) dv \right\}, \quad (30)$$

and

$$\zeta_{eq} = \zeta_n \frac{\omega_n}{\omega_{eq}} + \left(\frac{\omega_n}{\omega_{eq}} \right)^2 \frac{1-a}{\sqrt{\pi\theta}} \left(1 - \operatorname{erf}\left(\frac{1}{\sqrt{\theta}}\right) \right), \quad (31)$$

where

$$\theta = 2 \frac{\lambda_{eq,0,G}}{x_y^2}. \quad (32)$$

As in the previous case considered, iterations need to be performed to numerically derive equivalent linear properties ω_{eq} and ζ_{eq} , from Equations (20), and (30) to (32) to approximate statistically the response of a certain bilinear hysteretic oscillator defined by the parameters ω_n , ζ_n , a , and x_y or equivalently R (see Figure 3(b)), excited by a specific design spectrum compatible $G(\omega)$. Note that in this case the equivalent damping expression (Equation (31)) includes an additional term which accounts for the energy dissipation in the nonlinear system due to hysteresis.

4. NUMERICAL APPLICATION TO THE EC8 DESIGN SPECTRUM

4.1. EC8 design spectrum compatible power spectra

Consider the pseudo-acceleration design spectrum prescribed by the European aseismic code provisions (EC8) for soil conditions B, damping ratio $\zeta_n=5\%$, and peak ground acceleration equal to 36% the acceleration of the gravity (gray thick line in Figure 4(b)) as the given/ target spectrum [2]. Figure 4(a) includes discrete power spectra compatible with this target spectrum computed by means of Equation (7) for the three input spectral shapes $N(\omega)$ considered in section 2, namely white noise (WN) (Equation (10)), Kanai-Tajimi (KT) (Equation (11)), and Clough-Penzien (CP) (Equation (12)). The duration T_s is taken equal to 20sec, while the discretization step is set equal to $\Delta\omega=0.1\text{rad/sec}$. The requisite parameters for the definition of the KT and CP $N(\omega)$ spectra used are $\zeta_g=0.78$, $\omega_g=13.18\text{rad/sec}$, $\zeta_f=0.88$, and $\omega_f=3.13\text{rad/sec}$ reported in a recent work by [8]. These values pertain to a parametric CP type evolutionary power spectrum compatible with the herein considered EC8 target spectrum. Furthermore, Figure 4(a) shows an iteratively modified power spectrum computed by means of Equation (15) after four iterations assuming as the “seed” spectrum the aforementioned WN based spectrum which is the simplest and computationally least demanding case of a spectrum that can be obtained utilizing Equation (7).

Figure 4.

The associated with the above power spectra pseudo-acceleration response spectra calculated analytically by Equations (1) to (5) are plotted in Figure 4(b) and compared with the

target spectrum. As it can be seen in the latter figure, consideration of more elaborate input spectral shapes $N(\omega)$ in Equation (7) results in somewhat different power spectra attaining response spectra which achieve slightly better matching with the target design spectrum. Similar results can be found in Giaralis [56] for EC8 design spectra pertaining to all soil types as prescribed by the European aseismic regulations. However, the iteratively matched power spectrum which attains a notably more resonant (“spiky”) shape compared to the power spectra computed from Equation (7) without any additional iterations performed, achieves the best agreement with the target spectrum. More importantly, this iteratively modified WN based spectrum is computationally less costly to obtain compared to the KT and the CP based spectra considered herein which involve the calculation of more complex response spectral moments as it has been discussed in section 2 (see also [36, 39]). Thus, in the context of an efficient algorithmic determination of design spectrum compatible power spectra, it is suggested to perform a reasonable number of iterations via Equation (15); as a “seed” (i.e. initial estimate) a non-parametric power spectrum obtained from Equation (7) assuming a WN $N(\omega)$ spectrum can be used.

In Figure 4(c), pertinent results are shown associated with a Monte Carlo analysis conducted to assess the achieved level of compatibility of the aforementioned modified power spectrum with the target spectrum in terms of the criterion posed by Equation (1) for $p= 0.5$ (see also section 2). Specifically, an ensemble of 1000 stationary signals of 20sec duration each compatible with the iteratively modified power spectrum of Figure 4(a) are generated using an auto-regressive-moving-average (ARMA) filtering technique [57]. The response spectra of these signals are calculated [58] and the median spectral ordinates are compared with the EC8 target design spectrum in Figure 4(c). The cross-ensemble minimum and maximum spectral ordinates

are also included to illustrate the statistical nature of the analysis. Evidently, the criterion posed by Equation (1) is satisfactorily met, within engineering precision, by the iteratively modified power spectrum.

4.2. Equivalent linear systems and assessment via Monte Carlo analyses

In this subsection, the applicability of the proposed approach to estimate the maximum deformations of various stiffening piecewise linear elastic and bilinear hysteretic SDOF oscillators is illustrated. To this aim, the iteratively modified power spectrum of Figure 4(a) is used as a surrogate for determining equivalent linear systems (ELS) of natural period T_{eq} and of ratio of critical damping ζ_{eq} associated with the aforementioned nonlinear oscillators in the context of the statistical linearization method. Furthermore, Monte Carlo simulations pertaining to an ensemble of 40 non-stationary artificial accelerograms compatible with the previously defined EC8 design spectrum are conducted. This is done to confirm that the average peak response of the nonlinear systems compares reasonably well with those of the ELS. As shown in Figure 5 the ensemble average pseudo-acceleration spectrum of these accelerograms seismic signals is in a quite close agreement with the considered EC8 spectrum. These seismic signals have been generated by a wavelet-based stochastic approach recently proposed by the authors [8].

Figure 5.

In particular, Figure 6(a) to Figure 6(f) provide the properties of the ELSs (T_{eq} and ζ_{eq}) obtained by iteratively solving Equations (20), (25), and (26) for piecewise linear oscillators.

This is done for various yielding displacements x_y , natural periods T_n , rigidity ratios α , and for a fixed ratio of critical damping $\zeta_n = 0.05$ exposed to the iteratively modified power spectrum of Figure 4(a). Note that these properties are plotted against the ductility μ since this a normalized quantity of interest expressing the demand of structural performance imposed by the input seismic action in aseismic design practice (see also Figure 3). For the purposes of this study the ductility μ is computed as the ratio of the average peak response of each ELS exposed to the ensemble of the seismic signals of Figure 5 over the yielding displacement x_y of the corresponding non-linear system. As expected, systems of the same rigidity ratio α exhibiting more severe non-linear behavior in terms of higher ductility demand, or systems of the same level of ductility demand characterized by a higher rigidity ratio α yield stiffer ELS (i.e. ELS of decreased natural period T_{eq}). The equivalent viscous damping ζ_{eq} changes accordingly since by definition it is dependent on the natural frequency of the ELS (see also Equation (26)).

In Figure 6(g) to Figure 6(i) the aforementioned ductility demands are plotted for each considered ELS (lines of various types) versus the strength reduction factor R defined in Figure 3. These R factors are computed as the ratio of the average peak response of the infinitely linear system corresponding to the various considered T_n values excited by the aforementioned ensemble of signals over the yielding force f_y of the corresponding non-linear system (see also Figure 3a). Moreover, in Figure 6(g) to Figure 6(i) the average ductility demand μ obtained via numerical integration of the considered non-linear systems with piecewise linear restoring force (dots of various shapes) subject to the ensemble of the accelerograms of Figure 5 are also included. For this task, the standard constant acceleration Newmark's method, incorporating an iterative Newton-Raphson algorithm to treat locally the discontinuities of the piecewise linear force-deformation law, has been used (see e.g. [1]).

In general, the R - μ - T_n relations of Figure 6(g) to Figure 6(i) derived from the ELS and from the corresponding systems with piecewise linear type of stiffness nonlinearity as described above compare well for the cases considered. Clearly, this fact demonstrates the reliability of the ELS obtained via the proposed approach to estimate the peak deformations of the non-linear systems subject to seismic action defined by means of the given design spectrum.

Figure 6.

Similarly to the case of the piecewise linear oscillators, equivalent linear properties corresponding to bilinear hysteretic oscillators have been determined. This has been done for bilinear oscillators of various yielding displacements x_y , natural periods T_n , and for $\zeta_n = 0.05$ excited by the iteratively modified EC8 compatible power spectrum of Figure 4(a). The obtained equivalent linear properties are plotted in Figure 7(a) and Figure 7(b) versus the ductility μ . The rigidity ratio α is taken equal to 0.5. These properties have been derived by iteratively solving Equations (20) and (30) to (32). As one should expect vis a vis the previous case of the stiffening nonlinear elastic systems, for this “softening” system the stiffness of the ELSs decreases (increased T_{eq} values) for higher levels of nonlinearity as expressed by larger strength reduction factors R . Further, the departure from the region of linear response for this system leads to a significant increase of the viscous damping ratio of the ELSs to account for the additional energy dissipation achieved via the exhibited hysteretic behavior. Moreover, Figure 7(c) present R - μ - T_n relations based on averaged response time-histories obtained via numerical integration of the considered bilinear hysteretic systems (dots of various shapes) and of the corresponding ELSs (lines of various types) considering as input the ensemble of the seismic signals of Figure 5. An

algorithm similar to the one adopted in the case of the piecewise linear oscillators has been used to integrate the governing equation of the bilinear hysteretic systems.

Figure 7.

Clearly, the quality of the agreement between the peak response of the nonlinear systems and that of the ELSs deteriorates as the level of the nonlinearity increases. This is because the response of a system exhibiting strongly nonlinear behavior deviates significantly from a Gaussian and narrowband process even for Gaussian excitation; this attribute is not in conformity with the assumptions of the herein adopted statistical linearization method (see e.g. [9], [45]).

4.3. Estimation of peak nonlinear responses from elastic response spectra

Figure 8 and 9 include certain examples illustrating the manner by which the effective linear properties of the ELSs derived from the proposed approach can be used to approximate the peak responses of the associated nonlinear systems in terms of pseudo-acceleration spectral ordinates. Specifically, with reference to a certain elastic design spectrum for damping ζ_n and considering a specific nonlinear oscillator of natural period T_n for small oscillations (vertical dotted lines), one can move, following the horizontal arrows, to a vertical solid line which corresponds to an ELS characterized by $T_{eq} = 2\pi/\omega_{eq}$ and ζ_{eq} obtained by the proposed statistical linearization method and “read” the related spectral ordinate from an elastic design spectrum corresponding to the ζ_{eq} damping ratio. The equivalent linear T_{eq} and ζ_{eq} properties utilized in Figure 8 and Figure 9 are taken from the plots in Figure 6 and Figure 7, associated with the

various piecewise linear elastic and bilinear hysteretic oscillators considered, respectively. Obviously, in every case the aforementioned procedure for estimating maximum nonlinear responses from elastic design spectra can be facilitated by having available a collection of elastic design spectra corresponding to various levels of viscous damping. In this regard, it is noted that common code provisions typically include semi-empirical formulae calibrated from extensive Monte Carlo analyses to define elastic response spectra of various damping levels. (see e.g. [2]). However, the reliability of such formulae is still a matter of open research (e.g. [59, 60]). To this end, the response spectra of Figure 8 and Figure 9 corresponding to various damping ratios have been numerically computed [58] from the ensemble of the 40 accelerograms compatible to the 5%-damped design spectrum of Figure 5.

Figure 8.

Figure 9.

Note that the response spectra curves of the aforementioned figures corresponding to various ζ_{eq} damping ratios are amenable to a dual interpretation. Specifically, they can be construed both as elastic response spectra characterizing linear oscillators of increased viscous damping compared to the initial $\zeta_n=5\%$ in all examples herein considered. They can also be construed and as constant-strength inelastic response spectra corresponding to certain force reduction ratios R (see also [10, 12]). Focusing on the case of the bilinear hysteretic systems, and taking advantage of the aforementioned dual interpretation it is possible to develop constant-strength and constant-ductility inelastic spectra associated with a given design spectrum [1] from the $R-\mu-T_n$ relations of Figure 7 derived by integrating only the equivalent linear SDOF systems.

Certain examples are given in Figure 10. Interestingly, the influence of the initial value of T_n on the equivalent linear viscous damping ratio is relatively insignificant as implied by Figure 7(b). Thus, it is reasonable to consider inelastic spectra obtained from elastic spectra averaged over oscillators of fixed α and R (or μ) properties for various T_n using the mean value of the derived equivalent linear damping ratios denoted by $\bar{\zeta}_{eq}$ in Figure 10. As it has been already pointed out, if reliable elastic spectra of various damping ratios are available, the above spectra can be constructed without the need to consider any real recorded or artificial accelerogram. Note that if such a family is not available, it is possible to estimate the peak response of the underlying ELS based on Equation (1). Namely, as a product of a peak factor calculated from Equation (5) times the standard deviation of the response of the ELS system computed from Equation (20).

Figure 10.

Incidentally, compared to the elastic response spectrum (gray line in Figure 10), the inelastic spectra of Figure 10 for the bilinear oscillator are much smoother. They possess less prominent peaks while their ordinates increase only mildly for relatively short periods and decrease monotonically for longer periods. These observations are consistent with results from usual Monte Carlo analysis of nonlinear systems involving large ensembles of real recorded accelerograms (see e.g. [61]).

5. CONCLUDING REMARKS

An approach has been presented for estimating the peak seismic response of nonlinear systems exposed to excitations specified by a given design spectrum. The proposed approach relies on first determining a power spectrum which is equivalent, stochastically, to the given design spectrum. A computationally efficient numerical algorithm has been used for this task. This power spectrum is next used to determine, via statistical linearization, effective natural frequency and damping coefficients for the considered nonlinear system. These coefficients are then utilized to estimate readily the peak seismic response of the nonlinear system using standard linear response spectrum techniques. Clearly, this practice can be facilitated by the availability of families of elastic design spectra prescribed for a wide range of damping ratios. Furthermore, this approach can serve for developing inelastic response spectra from a given elastic response/design spectrum without the need of integrating numerically the nonlinear equations of motion for selected strong ground acceleration time-histories.

Numerical data supporting the reliability of the proposed approach have been provided; they pertain to the piecewise linear elastic and to the bilinear hysteretic kinds of nonlinear systems in conjunction with the EC8 elastic design spectrum. Specifically, appropriately normalized peak responses of these oscillators excited by a specific EC8 design spectrum have been computed via the proposed approach. These data have been juxtaposed with results from Monte Carlo analyses involving direct numerical integration of the non-linear equations of motion for a suite of non-stationary ground acceleration time histories compatible with the same EC8 spectrum. The comparison has shown a reasonable level of agreement.

Note that the proposed approach can perhaps be extended to accommodate the incorporation of more sophisticated nonlinear hysteretic models to capture structural behavior in greater detail (e.g. [55]) through the consideration of more elaborate statistical linearization schemes (e.g. [9, 62]). Furthermore, it is pointed out that currently various deterministic linearization methods assuming harmonic input excitation (e.g. [19]) are commonly used in tandem with given elastic design spectra to derive equivalent linear systems (ELSs) iteratively from ideal SDOF bilinear hysteretic oscillators. This is done in the context of the non-linear static (pushover) method (e.g. [17, 18, 47]), and in various displacement based aseismic design procedures (e.g. [46, 48]). It is hoped that the herein proposed statistical linearization based approach can be a useful alternative to these conventional linearization methods. Clearly, it yields ELS whose properties are explicitly related to the physics of the structural dynamics problem as captured by the design spectra prescribed in contemporary aseismic code provisions. Obviously, further research work is warranted in this regard.

APPENDIX

Consider a discretized stationary power spectrum $G[\omega_q] = G_q$, where ω_q are equally spaced frequencies calculated as $\omega_q = \omega_0 + (q-0.5)\Delta\omega$; $q = 1, 2, \dots, M$ and ω_0 is given by Equations (8) and (9). By discretizing the frequency domain according to the grid: $\omega_p = \omega_0 + (p-1)\Delta\omega$; $p = 1, 2, \dots, M+1$, the first three response spectral moments of Equation (2) can be numerically evaluated using the formula [29, 31, 40]

$$\lambda_{n,m,G} = \sum_{p=1}^M J_{n,m,p} G_p, \quad (\text{A})$$

in which

$$\begin{aligned}
J_{n,m,p} = & \frac{x_1}{2} \ln \frac{(\omega_{p+1} - \omega_D)^2 + c^2}{(\omega_p - \omega_D)^2 + c^2} + \\
& \frac{x_2 + \omega_D x_1}{c} \left\{ \frac{\pi}{2} \left[1 - \operatorname{sgn} \left(\frac{c(\omega_{p+1} - \omega_p)}{(\omega_{p+1} - \omega_D)(\omega_p - \omega_D) + c^2} \right) \right] + \tan^{-1} \frac{c(\omega_{p+1} - \omega_p)}{(\omega_{p+1} - \omega_D)(\omega_p - \omega_D) + c^2} \right\} +, \quad (\text{B}) \\
& \frac{x_3}{2} \ln \frac{(\omega_{p+1} - \omega_D)^2 + c^2}{(\omega_p - \omega_D)^2 + c^2} + \frac{x_4 - \omega_D x_3}{c} \tan^{-1} \frac{c(\omega_{p+1} - \omega_p)}{(\omega_{p+1} + \omega_D)(\omega_p + \omega_D) + c^2}
\end{aligned}$$

where $\omega_D = \omega_n \sqrt{1 - \zeta_n^2}$, $c = \omega_n \zeta_n$, and

$$\begin{aligned}
\begin{Bmatrix} x_1 \\ x_2 \\ x_3 \\ x_4 \end{Bmatrix} = & \begin{bmatrix} -\frac{1}{4\omega_n^2 \omega_D} & 0 & \frac{1}{4\omega_D} \\ \frac{1}{2\omega_n^2} & \frac{1}{4\omega_D} & 0 \\ \frac{1}{4\omega_n^2 \omega_D} & 0 & -\frac{1}{4\omega_D} \\ \frac{1}{2\omega_n^2} & -\frac{1}{4\omega_D} & 0 \end{bmatrix} \begin{Bmatrix} r_0 \\ r_1 \\ r_2 \end{Bmatrix} ; \quad r_i = \begin{cases} 1, & i = m \\ 0, & i \neq m \end{cases} \quad (\text{C})
\end{aligned}$$

REFERENCES

- [1] A.K. Chopra, Dynamics of Structures. Theory and Applications to Earthquake Engineering, second ed., Prentice-Hall, New Jersey, 2001.
- [2] CEN. Eurocode 8: Design of Structures for Earthquake Resistance - Part 1: General Rules, Seismic Actions and Rules for Buildings, EN 1998-1: 2004, Comité Européen de Normalisation, Brussels, 2004.
- [3] A.S. Veletsos, N.M. Newmark, Effect of inelastic behavior on the response of simple systems to earthquake motions. Proc. 2nd World Conference on Earthquake Engineering, Japan, Vol. 2 (1960) 895–912.
- [4] N.M. Newmark, W.J. Hall, Earthquake Spectra and Design, Earthquake Engineering Research Institute, Berkeley, 1982.
- [5] E. Miranda, V.V. Bertero, Evaluation of strength reduction factors for earthquake-resistance design, Earthq. Spectra 10 (1994) 357-379.
- [6] B. Borzi, G.M. Calvi, A.S. Elnashai, E. Faccioli, J.J. Bommer, Inelastic spectra for displacement-based seismic design, Soil Dyn. Earthq. Eng. 21 (2001) 47-61.
- [7] A.K. Chopra, C. Chintanapakdee, Inelastic deformation ratios for design and evaluation of structures: Single-degree-of-freedom bilinear systems, J. Struct. Eng. ASCE 130 (2004) 1309-1319.
- [8] A. Giaralis, P.D. Spanos, Wavelet-based response spectrum compatible synthesis of accelerograms- Eurocode application (EC8), Soil Dyn. Earthq. Eng. 29 (2009): 219-235.
- [9] J.B. Roberts, P.D. Spanos, Random Vibration and Statistical Linearization, Dover Publications, New York, 2003.

- [10] W.D. Iwan, Estimating inelastic response spectra from elastic spectra, *Earthq. Eng. Struct. Dyn.* 8 (1980) 375–388.
- [11] W.D. Iwan, N.C. Gates, Estimating earthquake response of simple hysteretic structures, *J. Eng. Mech. Div. ASCE* 105 (1979) 391-405.
- [12] W.P. Kwan, S.L. Billington, Influence of hysteretic behavior on equivalent period and damping of structural systems, *J. Struct. Eng. ASCE* 129 (2003) 576-585.
- [13] P. Gulkan, M.A. Sozen, Inelastic responses of reinforced concrete structures to earthquake motions, *J. Am. Concr. Inst.* 71 (1974) 604-610.
- [14] A. Shibata, M.A. Sozen, Substitute-structure method for seismic design in R/C, *J. Struct. Eng. Div. ASCE* 102 (1976) 1-18.
- [15] M.J. Kowalsky, M.J.N. Priestley, G.A. MacRae, Displacement-based design of RC bridge columns in seismic regions. *Earthq. Eng. Struct. Dyn.* 24 (1995) 1623-1643.
- [16] G.M. Calvi, G.R. Kingsley, Displacement-based seismic design of multi-degree-of-freedom bridge structures. *Earthq. Eng. Struct. Dyn.* 24 (1995) 1247-1266.
- [17] P. Fajfar, A nonlinear analysis method for performance-based seismic design. *Earthq. Spectra* 16 (2000) 573-592.
- [18] A.K. Chopra, R.K. Goel, Evaluation of NSP to estimate seismic deformation: SDF systems, *J. Struct. Eng. ASCE* 126 (2000) 482-490.
- [19] P.C. Jennings, Equivalent viscous damping for yielding structures. *J. Eng. Mech. Div. ASCE* 94 (1968) 103-116.
- [20] W.D. Iwan, N.C. Gates, The effective period and damping of a class of hysteretic structures, *Earthq. Eng. Struct. Dyn.* 7 (1979) 199-211.
- [21] A.H. Hadjian, A re-evaluation of equivalent linear models for simple yielding systems, *Earthq. Eng. Struct. Dyn.* 10 (1982) 759-767.
- [22] P.K. Koliopoulos, E.A. Nichol, G.D. Stefanou, Comparative performance of equivalent linearization techniques for inelastic seismic design, *Eng. Struct.* 16 (1996) 5-10.
- [23] B. Basu, V.K. Gupta, A note on damage-based inelastic spectra, *Earthq. Eng. Struct. Dyn.* 25 (1996) 421-433.
- [24] B. Basu, V.K. Gupta, A damage-based definition of effective peak acceleration, *Earthq. Eng. Struct. Dyn.* 27 (1998) 503-512.
- [25] E. Miranda, J. Ruiz-García, Evaluation of approximate methods to estimate maximum inelastic displacement demands, *Earthq. Eng. Struct. Dyn.* 31 (2002) 539-560.
- [26] I. Politopoulos, C. Feau, Some aspects of floor spectra of IDOF nonlinear primary structures, *Earthq. Eng. Struct. Dyn.* 36 (2007) 975-993.
- [27] I.D. Gupta, M.D. Trifunac, Defining equivalent stationary PSDF to account for nonstationarity of earthquake ground motion, *Soil Dyn. Earthq. Eng.* 17 (1998) 89-99.
- [28] M.K. Kaul, Stochastic characterization of earthquakes through their response spectrum, *Earthq. Eng. Struct. Dyn.* 6 (1978) 497-509.
- [29] D.D. Pfaffinger, Calculation of power spectra from response spectra, *J. Eng. Mech. ASCE* 109 (1983) 357-372.
- [30] Y.J. Park, New conversion method from response spectrum to PSD functions, *J. Eng. Mech. ASCE* 121 (1995) 1391-1392.
- [31] P. Cacciola, P. Colajanni, G. Muscolino, Combination of modal responses consistent with seismic input representation, *J. Struct. Eng. ASCE* 130 (2004) 47-55.
- [32] T.K. Caughey, Random excitation of a system with bilinear hysteresis, *J. Appl. Mech. ASME* 27 (1960) 649-652.
- [33] S.H. Crandall, Is stochastic equivalent linearization a subtly flawed procedure?, *Probab. Eng. Mech.* 16 (2001) 169-176.
- [34] E.H. Vanmarcke, Structural response to earthquakes, in: C. Lomnitz, E. Rosenblueth (Eds.), *Seismic Risk and Engineering Decisions*, Elsevier, Amsterdam, 1976.
- [35] S.H. Crandall, First crossing probabilities of the linear oscillator, *J. Sound Vib.* 12 (1970) 285-299.
- [36] A. Der Kiureghian, Structural response to stationary excitation, *J. Eng. Mech. Div. ASCE* 106 (1980) 1195-1213.
- [37] K. Kanai, Semi-empirical formula for the seismic characteristics of the ground, *Univ. Tokyo Bull. Earthq. Res. Inst.* 35 (1957) 309-325.
- [38] R.W. Clough, J. Penzien, *Dynamics of Structures*, second ed., Mc-Graw Hill, New York, 1993.
- [39] P.D. Spanos, S.M. Miller, Hilbert transform generalization of a classical random vibration integral, *J. Appl. Mech. ASME* 61 (1994) 575-581.

- [40] M. Di Paola, L. La Mendola, Dynamics of structures under seismic input motion (Eurocode 8), *Eur. Earthq. Eng.* 6 II (1992) 36-44.
- [41] W.D. Iwan, E.J. Patula, The merit of different error minimization criteria in approximate analysis, *J. Appl. Mech. ASME* 39 (1972) 257-262.
- [42] A. Naess, Prediction of extreme response of nonlinear structures by extended stochastic linearization. *Probab. Eng. Mech.* 10 (1995) 153-160.
- [43] I. Elishakoff, Stochastic linearization technique: A new interpretation and a selective review, *Shock Vib. Dig.* 32 (2000) 179-188.
- [44] J.E. Hurtado, A.H. Barbat, Equivalent linearization of the Bouc-Wen hysteretic model. *Eng. Struct.* 22 (2000) 1121-1132.
- [45] Y.J. Park, Equivalent linearization for seismic responses. I: Formulation and error analysis, *J. Eng. Mech. ASCE* 118 (1992) 2207-2226.
- [46] C.A. Blandon, M.J.N. Priestley, Equivalent viscous damping equations for direct displacement based design, *J. Earthq. Eng.* 9 (special issue 2) (2005) 257-278.
- [47] M. Fragiocomo, C. Amadio, S. Rajgelj, Evaluation of the structural response under seismic actions using non-linear static methods, *Earthq. Eng. Struct. Dyn.* 35 (2006) 1511-1531.
- [48] H.M. Dwairi, M.J. Kowalsky, J.M. Nau, Equivalent damping in support of direct displacement-based design. *J. Earthq. Eng.* 11 (2007) 512-530.
- [49] A. Ruangrassamee, K. Kawashima, Control of nonlinear bridge response with pounding effect by variable dampers, *Eng. Struct.* 25 (2003) 593-606.
- [50] J.P. Wolf, P.E. Skrikerud, Mutual pounding of adjacent structures during earthquakes, *Nucl. Eng. Des.* 57 (1980) 253-275.
- [51] S.A. Anagnostopoulos, Pounding of buildings in series during earthquakes, *Earthq. Eng. Struct. Dyn.* 16 (1988) 443-456.
- [52] G.H. Powell, Seismic response analysis of above-ground pipelines, *Earthq. Eng. Struct. Dyn.* 6 (1978) 157-165.
- [53] H.-C. Tsai, Dynamic analysis of base-isolated shear beams bumping against stops, *Earthq. Eng. Struct. Dyn.* 26 (1997) 515-528.
- [54] O.M. Ramirez, M.C. Constantinou, J.D. Gomez, A.S. Whittaker, C.Z. Chrysostomou, Evaluation of simplified methods of analysis of yielding structures with damping systems, *Earthq. Spectra* 18 (2002) 501-530.
- [55] Y. Suzuki, R. Minai, Application of stochastic differential equations to seismic reliability analysis of hysteretic structures. *Probab. Eng. Mech.* 3 (1998) 43-52.
- [56] A. Giaralis, Wavelet based response spectrum compatible synthesis of accelerograms and statistical linearization based analysis of the peak response of inelastic systems. Ph.D. Thesis. Dept of Civil and Environmental Engineering, Rice University, Houston, 2008.
- [57] P.D. Spanos, B.A. Zeldin, Monte Carlo treatment of random fields: A broad perspective, *Appl. Mech. Rev.* 51 (1998) 219-237.
- [58] N.C. Nigam, P.C. Jennings, Calculation of response spectra from strong-motion earthquake records, *Bull. Seismol. Soc. Am.* 59 (1969) 909-922.
- [59] S.V. Tolis, E. Faccioli, Displacement design spectra, *J. Earthq. Eng.* 3 (1999) 107-125.
- [60] Y.Y. Lin, E. Miranda, K.-C. Chang, Evaluation of damping reduction factors for estimating elastic response of structures with high damping, *Earthq. Eng. Struct. Dyn.* 34 (2005) 1427-1443.
- [61] S. Jarenprasert, E. Bazán, J. Bielak, Inelastic spectrum-based approach for seismic design spectra, *J. Struct. Eng. ASCE* 132 (2006) 1284-1292.
- [62] Y.K. Wen, Equivalent linearization for hysteretic systems under random excitation, *J. Appl. Mech. ASME* 47 (1980) 150-154.

Figures with captions

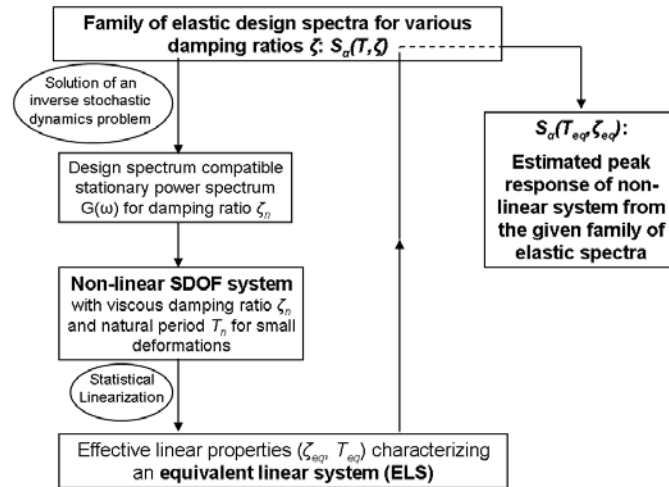


Figure 1. Flowchart of the proposed approach.

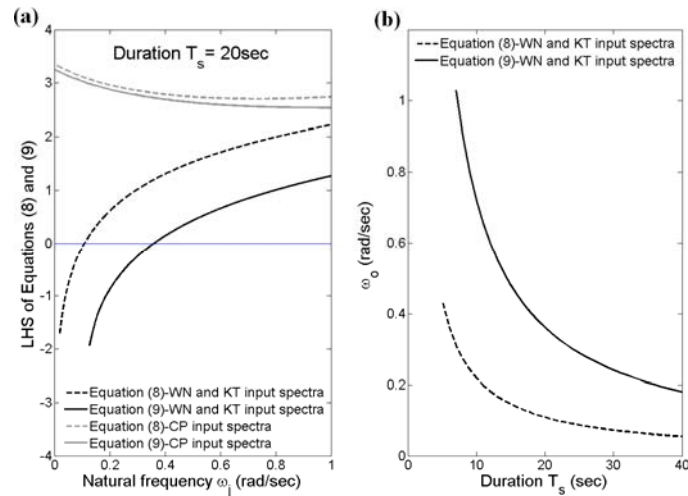


Figure 2. Numerical evaluation of the conditions posed by Equations (8) and (9) and determination of the frequency ω_0 appearing in Equation (7) for several values of the duration T_s of the underlying stationary process characterized by the $N(\omega)$ spectrum taken as WN (Equation (10)), KT (Equation (11) for $\omega_g = 15$ rad/sec; $\zeta_g = 0.6$), and CP (Equation (12) for $\omega_g = 15$ rad/sec; $\zeta_g = 0.6$; $\omega_f = 3$ rad/sec; $\zeta_f = 1$).

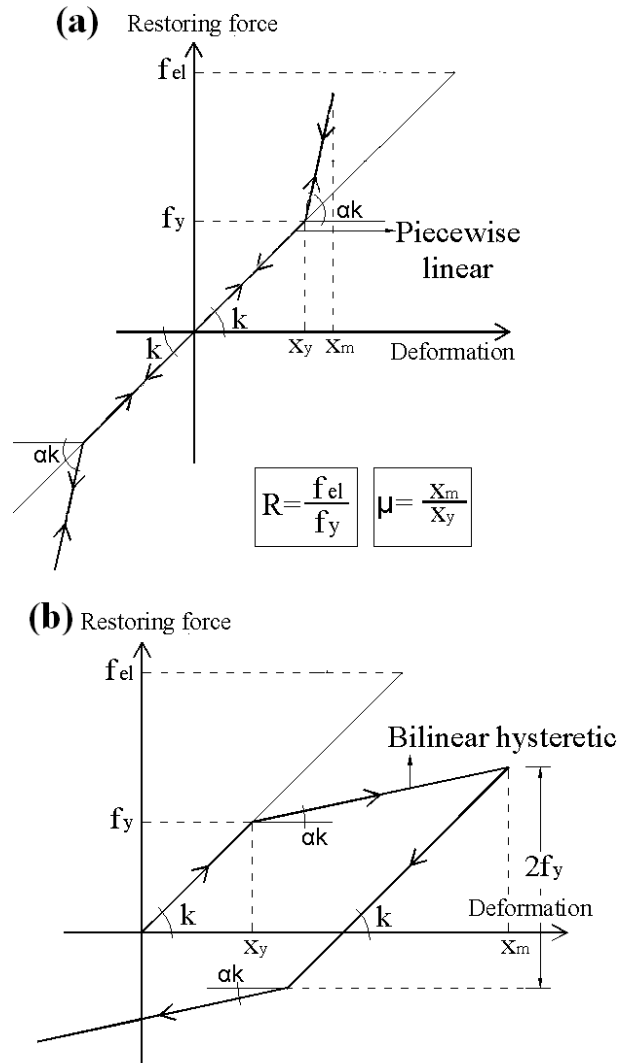


Figure 3. Nonlinear restoring force-deformation laws considered and definitions of the strength reduction factor R and ductility μ . (a) Two-brunch piecewise elastic restoring force functions. (b) Bilinear hysteretic restoring force.

The symbol k denotes the stiffness of the infinitely linear system associated with the response of the non-linear systems in the range of small deformations.

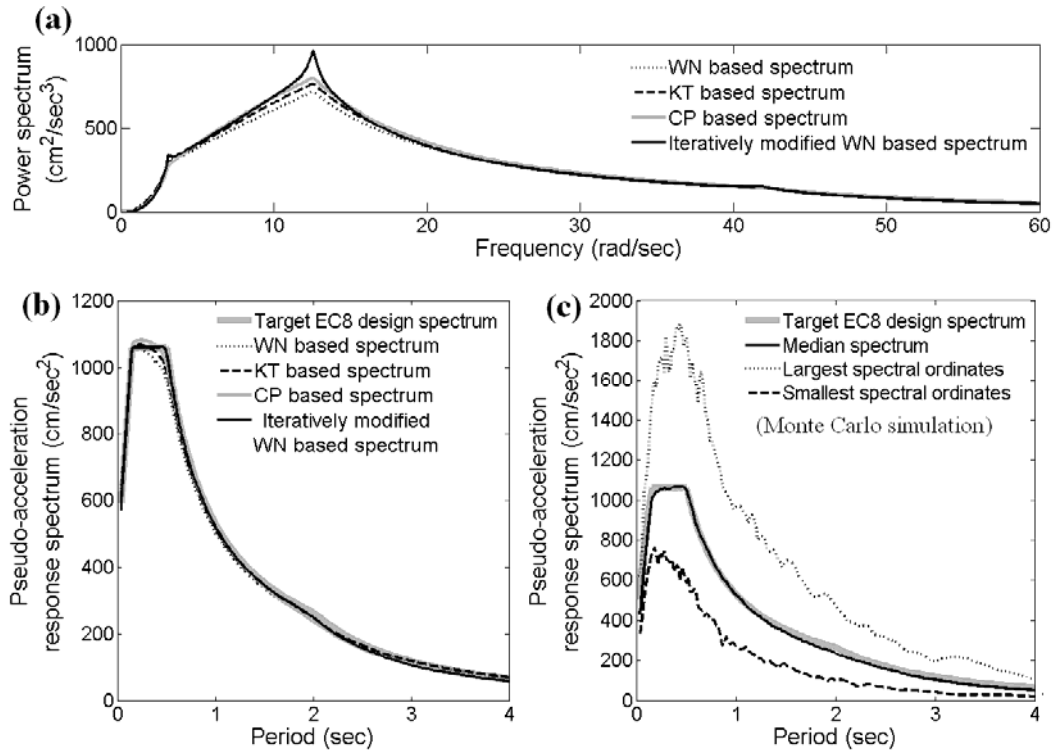


Figure 4. (a) Power spectra obtained by Equation (7) for various input spectra $N(\omega)$ and an iteratively modified spectrum obtained by Equation (15) after 4 iterations compatible with the target EC8 design spectrum ($\zeta=5\%$; $PGA=0.36g$; soil conditions B). (b) Response spectra calculated by Equation (1) pertaining to the power spectra of panel (a). (c) Numerical verification of the compatibility criterion posed by Equation (1) for the iteratively matched spectrum of panel (a).

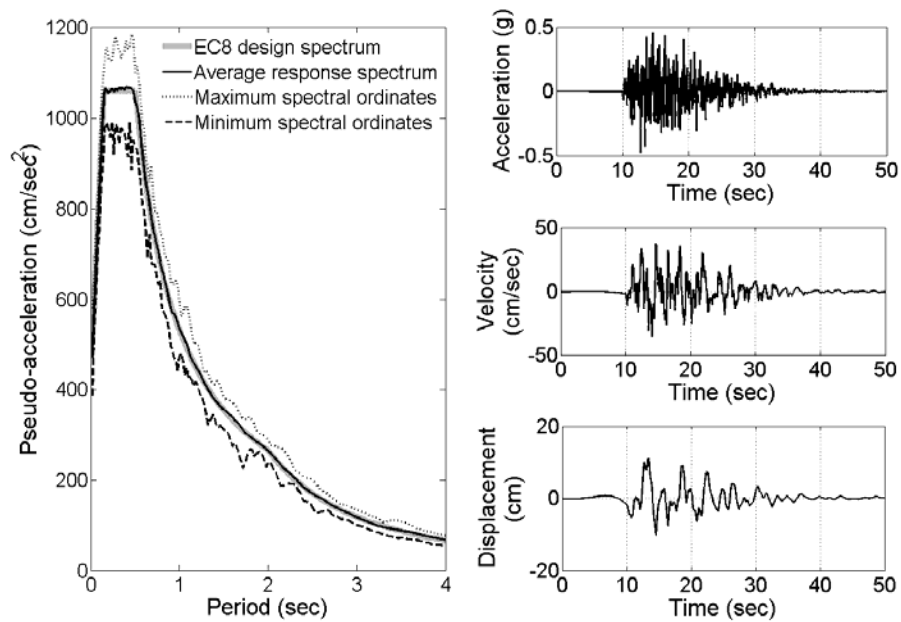


Figure 5. Response spectra of an ensemble of 40 artificial non-stationary accelerograms compatible with the target EC8 design spectrum. The time-history of one of these accelerograms and its corresponding velocity and displacement trace are also plotted.

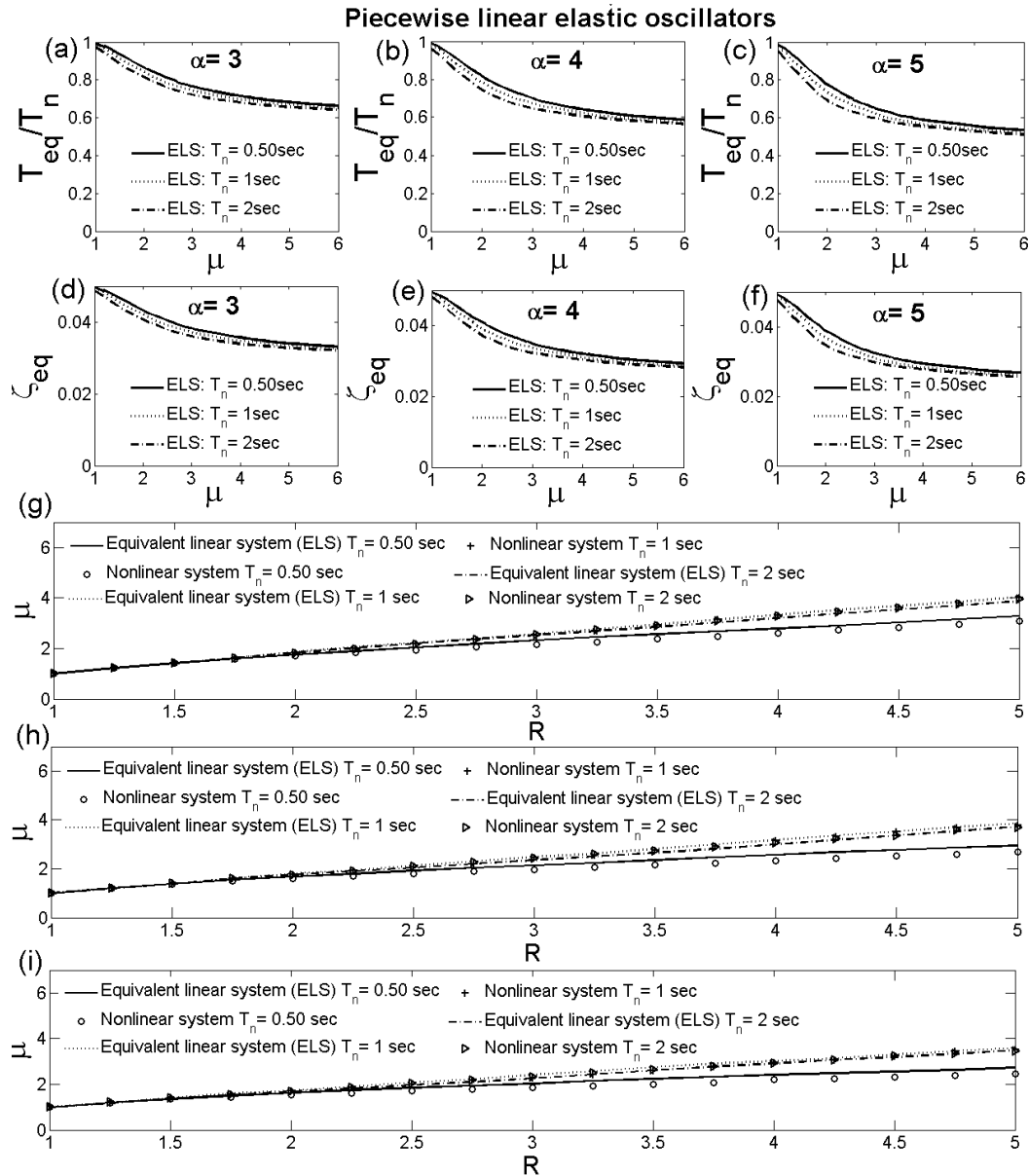


Figure 6. (a) to (f): Effective properties of ELSs corresponding to various viscously damped oscillators with piecewise linear elastic restoring force-deformation law compatible with the considered EC8 design spectrum. (g) to (i): Evaluation of the potential of the derived ELSs to estimate the peak response of the considered nonlinear oscillators via Monte Carlo simulations.

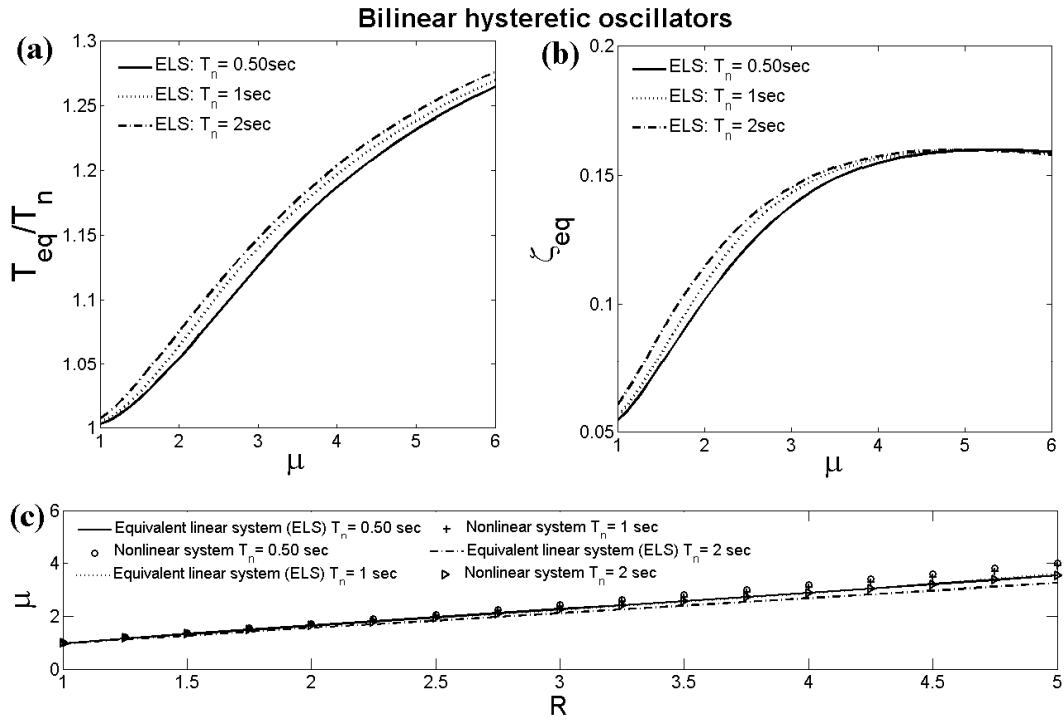


Figure 7. (a) to (b): Effective properties of ELSs corresponding to various viscously damped oscillators with bilinear hysteretic restoring force-deformation law ($\alpha=0.5$) compatible with the considered EC8 design spectrum. (c): Evaluation of the potential of the derived ELSs to estimate the peak response of the considered nonlinear oscillators via Monte Carlo simulations.

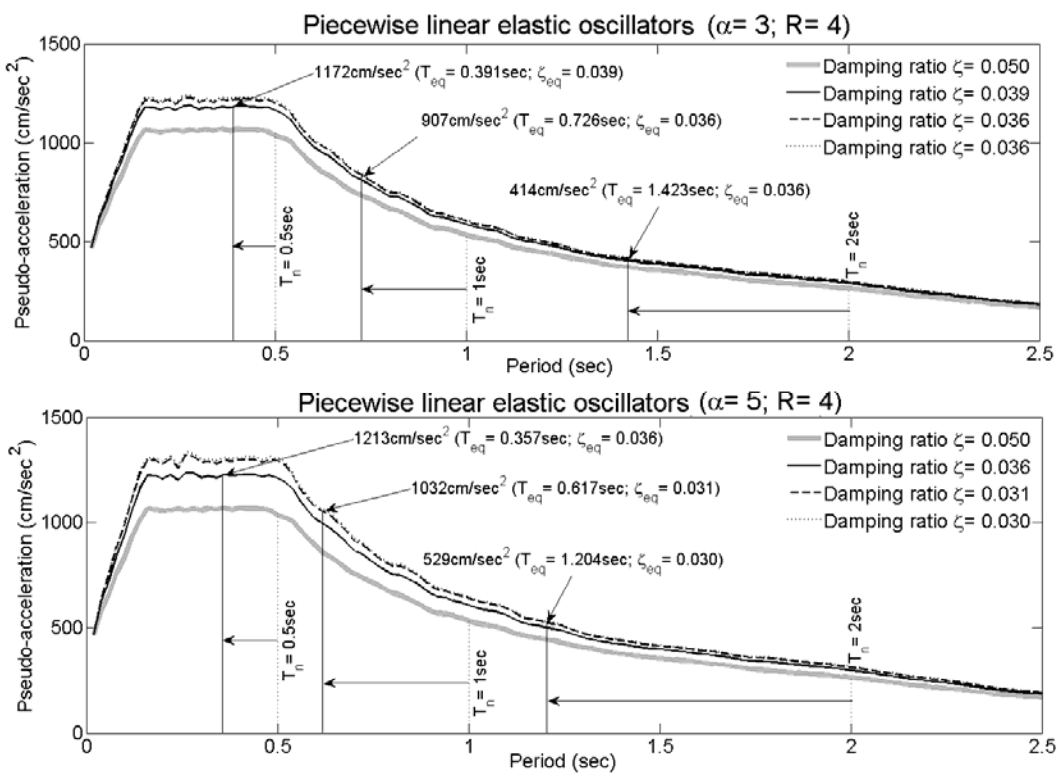


Figure 8. Estimation of maximum response of various non-linear oscillators following a piecewise linear elastic restoring force-deformation law from elastic design spectra in terms of pseudo-acceleration.

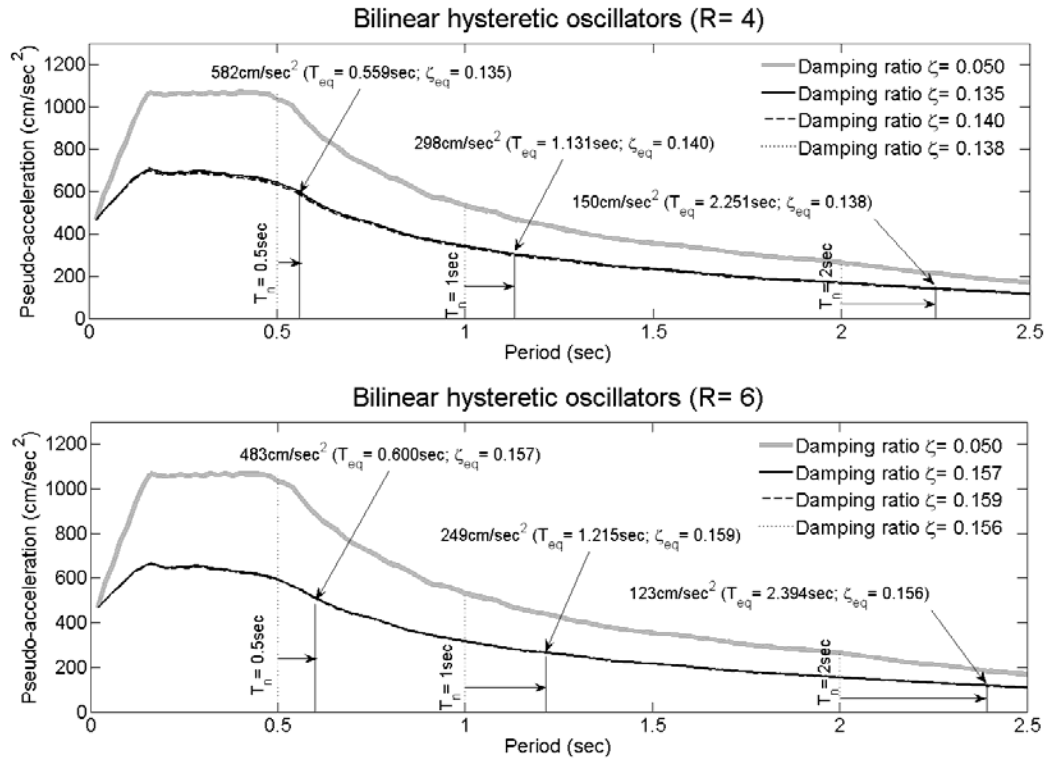


Figure 9. Estimation of maximum response of various non-linear oscillators following a bilinear hysteretic restoring force-deformation law ($\alpha=0.5$) from elastic design spectra in terms of pseudo-acceleration.

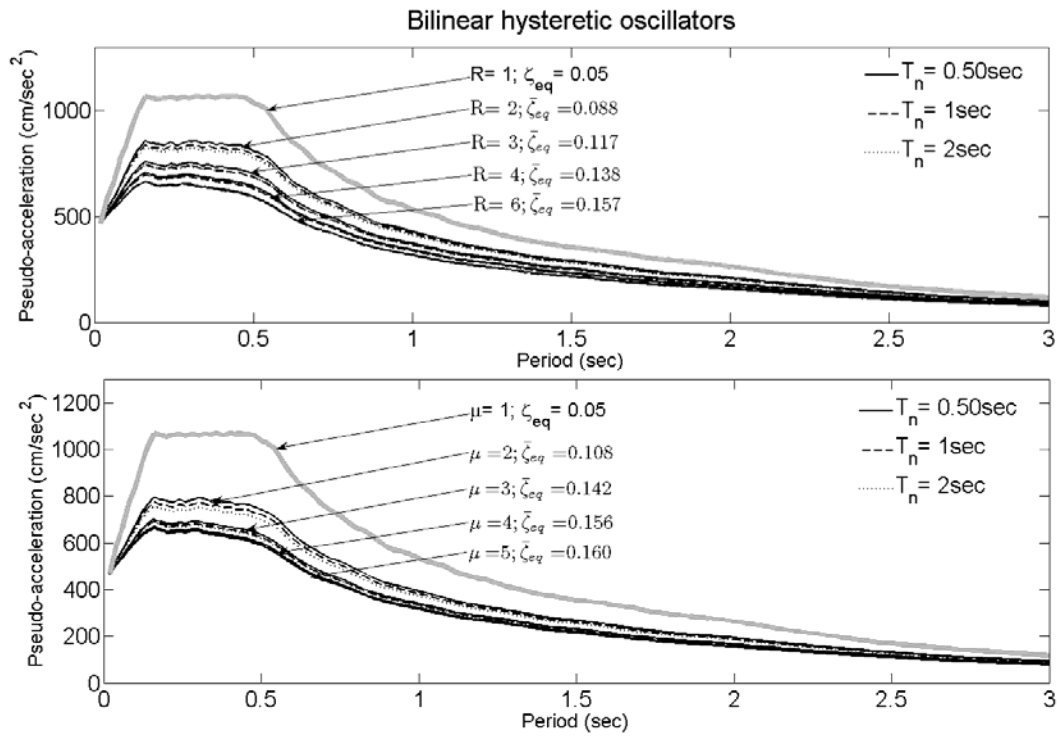


Figure 10. Estimated constant strength and constant ductility inelastic spectra from elastic spectra for various bilinear hysteretic oscillators ($\alpha=0.5$).